Molecular and Cellular Biochemistry 51, 79–95(1983)

Subsite structure and ligand binding mechanism of glucoamylase

Keitaro Hiromi, Masatake Ohnishi and Akiyoshi Tanaka
Department of Food Science and Technology, Faculty of Agriculture, Kyoto University, Kyoto 606, Japan

Summary

1. The basic concept and outline of the subsite theory were described, which correlates quantitatively the subsite structure (the arrangement of subsite affinities) to the action pattern of amylases in a unified manner.

2. The subsite structures of several amylases including glucoamylase were summarized.

3. In parallel with the theoretical prediction obtained therefrom, the binding subsites of glucose, gluconolactone and linear substrates to *Rhizopus* glucoamylase were investigated experimentally, by using steady-state inhibition kinetics, difference absorption spectrophotometry, and fluorometric titration.

4. From several lines of evidence, it was concluded that gluconolactone, a transition state analogue, is bound at Subsite 1 (nonreducing end side) where a tryptophan residue is located.

5. The stopped-flow kinetic studies have revealed that all the ligand bindings studied consist of two-step mechanism in which a bimolecular association between the enzyme and a ligand to form a loosely bound complex (EL) followed by the unimolecular isomerization process in which EL converts to the final firmly bound EL* complex. For substrates the EL* may be the productive complex and the fluorescence of the tryptophan located at Subsite 1 is quenched in their isomerization process, most probably a relocation of ligand to occupy this subsite.

Introduction

The concept of subsite emerged originally from proteases (1, 2). Each amino acid side chain of a substrate is assumed to interact with an individual 'subsite', a part of the active site of the enzyme, with a certain 'affinity'. The arrangement of such subsites, termed 'subsite structure', will determine the specificity of the protease concerned. In this case, however, the 'subsite affinity', the decrease in the unitary binding free energy at a subsite, depends on the amino acid side chain to be bound at the subsite, and hence a definite value cannot be assigned for each subsite. In homopolymer-degrading enzymes, the situation is much simpler. Since the component residue of a substrate is identical, only one subsite affinity can be assigned for a given subsite. This facilitates a unified and quantitative theoretical treatment of the action pattern of a homopolymer-degrading enzyme a great deal.

Among a limited number of homopolymer-degrading enzymes, amylase may be the best suited one, since a variety of amylases with different action patterns have been crystallized, soluble substrates of different degrees of polymerization (DP) are readily available, and most amylases have little or no transferring activity, which makes the systematic study much easier than, for example, cellulase and lysozyme.

In these ten years, we have been involved in theoretical and experimental studies for analyzing quantitatively action patterns of several amylases in terms of their subsite affinities, focusing attention to the following two main action patterns; the de-

pendence of hydrolytic rate on DP of linear substrates and the cleavage pattern of maltooligosaccharides. The basic idea is that these action patterns of amylases are determined by their subsite structures, i.e., the arrangements of subsite affinities, and conversely the subsite affinities of an amylase can be determined from the analysis of its action pattern; i.e., by studying the DP dependence of Michaelis parameters and the mode of cleavage of end-labeled maltooligosaccharides quantitatively. The knowledge of subsite structure is useful in the interpretation of substrate specificity (3), in the theoretical prediction of time course of product distribution (4), and in characterizing (or exploring the nature of) subsites (5–8).

If we regard a subsite as a structural unit constituting the enzyme active site, the subsite theory provides us with a useful means for studying the 'structure-function relationship' of amylases quantitatively in terms of a subsite. This approach must be valuable especially for those enzymes, such as amylases (except for Taka-amylase A (9, 10)), whose three-dimensional structures have not been determined yet.

Glucoamylase, which is one of the best used enzymes, has a simple action pattern splitting off glucose from nonreducing ends of starch (11). *Rhizopus* glucoamylase is the first enzyme to which the subsite theory was successfully applied (12–14). The subsite structure thus determined enabled us to predict binding modes of substrates and analogues and to calculate the time course of product distribution. Based on these informations, static and kinetic studies have been done, combined with fast reaction techniques and chemical modification, to elucidate the nature of subsites and mechanisms of the interaction between the enzyme and substrates and analogues. In this review, we would like to outline the subsite theory and its application to the above subjects.

Materials and methods

Glucoamylases from *Rhizopus delemar* and *Rhizopus niveus* are of pure grade samples purchased from Seikagaku Kogyo, Co. Ltd. In some experiments a major fraction of five isozymes included in the preparations was used, which was prepared by the ion-exchange chromatography and the preparative isoelectric focusing method (15). No essential differences in the enzymatic properties have been found between the fractionated and the unfractionated preparations. Maltooligosaccharides were prepared from cycloheptaamylose as described elsewhere (16). Other substrates, analogues and chemicals were of commercial origins of guaranteed grade.

For the methods employed, including steady-state kinetic studies, difference absorption spectrophotometry, fluorometry, and stopped-flow kinetic studies on ligand binding and chemical modification, our original papers cited at relevant portions are to be referred to. Reaction conditions etc. are described in the figure legends. Unless otherwise stated, pH was 4.5 with 0.02 M acetate buffer.

Outline of subsite theory

When there are a number of binding modes of a linear n-mer substrate S_n with an amylase E (see Fig. 1), the Michaelis-Menten scheme should be written as follows:

$$E + S_n \underset{}{\overset{K_{n,p}}{\rightleftharpoons}} ES_{n,p} \xrightarrow{k_{int}} E + P \qquad (1)$$

$$S_n \xrightarrow{K_{n,q}} ES_{n,q}$$

where $K_{n,p}$ and $K_{n,q}$ represent the binding constants between E and S_n to form productive enzyme-substrate complex(es), $ES_{n,p}$, and nonproductive complexes, $ES_{n,q}$, respectively, and k_{int} designates the rate constant of glucoside bond cleavage in every productive complex, which is assumed constant irrespective of the length of the substrate, n. This assumption is quite reasonable in chemical sence, since the rate constant for acid catalyzed hydrolysis of glucoside bond is almost independent of the DP (= n) of substrates (17). If we use a subscript j for specifying a particular binding mode (including productive and nonproductive modes, designated by p and q, respectively), a general expression for a binding constant $K_{n,j}$ is given by

$$K_{n,j} = [ES_{n,j}]/[E][S] \qquad (2)$$

where $ES_{n,j}$ is the enzyme-substrate complex either productive or nonproductive, in the j-th binding

mode. Conveniently j is taken equal to the subsite number of a subsite which is occupied by the nonreducing end glucose residue of a substrate (see Fig. 1).

From the scheme of Eq. 1, we have the following steady-state rate equation of exactly the same form as the well-known Michaelis-Menten equation which relates the initial rate v with the substrate concentration $[S_n]$;

$$v = \frac{k_0[E]_0[S_n]}{K_m + [S_n]} \tag{3}$$

where k_0 is the molecular activity and K_m is the Michaelis constant. The meanings of K_m and k_0, however, are not so simple as those of the conventional Michaelis-Menten scheme, but they are given as follows (12–14):

$$1/K_m = \sum_j K_{n,j} = \sum_p K_{n,p} + \sum_q K_{n,q} \tag{4}$$

$$k_0 = k_{int} \frac{\sum_p K_{n,p}}{\sum_p K_{n,p} + \sum_q K_{n,q}} = \frac{k_{int}}{1 + (\sum_q K_{n,q} / \sum_p K_{n,p})} \tag{5}$$

and hence

$$k_0/K_m = k_{int}(\sum_p K_{n,p}) \tag{6}$$

where $\sum_p$, $\sum_q$, and $\sum_j$ indicate that the sum is taken for the productive, the nonproductive, and the both complexes, respectively. It should be noted that k_0/K_m has the productive terms only, whereas either K_m or k_0 contains nonproductive terms as well as productive ones.

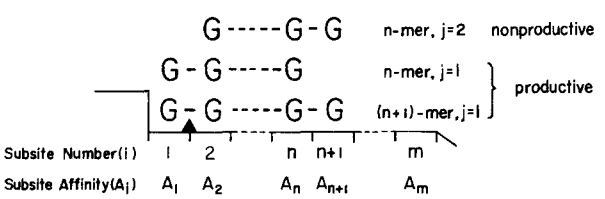

Fig. 1. Schematic representation of the active site of glucoamylase and the binding modes of n-mer and (n + 1)-mer substrates. G represents a glucose residue of a substrate. The wedge indicates the catalytic site of the enzyme. Subsites are numbered counting from the terminal one to which nonreducing end glucose residue of substrates is situated in the productive binding mode. The binding modes with j = 1 and j = 2 refer to productive and non-productive complexes, respectively.

We assume that an amylase has m subsites each of which has its own subsite affinity, A_i, i being the number of a subsite counting from the terminal one on the nonreducing end side. Then the unitary part of the binding affinity (or the unitary part of the negative standard free energy change for the binding), termed 'molecular binding affinity', B_n, of an n-mer substrate in a particular binding mode j, can be given as follows:

$$B_{n,j} = (\overset{\text{cov.}}{\sum_i} A_i)_{n,j} = RT \ln K_{n,j} + 2.4 \text{ kcal/mol} \quad (\text{at } 25\,^\circ\text{C}) \tag{7}$$

where $\overset{\text{cov.}}{\sum_i} A_i$ indicates that the sum of A_i is taken for all the subsites covered by the substrate S_n in the j-th binding mode, and 2.4 kcal/mol is a correction term arising from the difference in the mixing entropies between the initial and the final states.

Thus when the A_i value of every subsite is known, we can readily estimate the binding constant $K_{n,j}$ for any linear substrate in a given binding mode, according to the following equation derived from Eq. 7;

$$K_{n,j} = 0.018 \exp(\overset{\text{cov.}}{\sum_i} A_i)_{n,j} \tag{8}$$

In this way, the probability of occurrence of a given binding mode of a substrate can be predicted easily from the arrangement of the subsite affinities, i.e., the 'subsite structure', of an amylase.

By substituting Eq. 8 into Eqs. 4–6, all the Michaelis parameters, K_m and k_0 (and also k_0/K_m), can be expressed in terms of one rate constant, k_{int}, and m subsite affinities, A_i's, i.e., in total (m + 1) 'subsite parameters'. (The complete equations will not be written here.) Conversely one can determine the values of A_i's and k_{int} from the DP dependence of K_m and k_0 (12–14).

The essence of the subsite theory stated above tells us the following:

1) The Michaelis constant K_m decreases, or the apparent 'affinity' increases, with increasing chain length of substrate, since both the number of binding modes (productive and nonproduc-

tive) and that of occupied subsites (and hence the sum of A_i's) increase with DP.

2) The molecular activity, k_0, is proportional to the fraction of productive binding terms out of total (productive and nonproductive) binding terms. In other words, the ratio between the sums of the nonproductive and the productive terms ($\sum_q K_{n,q} / \sum_p K_{n,p}$) determines the magnitude of k_0 (see Eq. 5). And for this reason k_0 can be DP dependent. Since the A_i value would be negative for a subsite adjacent to the catalytic site due to the distortion of glucose residue bound at the subsite (as evidenced in the case of lysozyme (18–21), the smallest substrate maltose may well have low probability of productive binding and hence low k_0 value. This is the case for amylases in general. When the productive terms overwhelm the nonproductive ones, k_0 becomes equal to k_{int}, which is assumed to be DP independent. This situation actually occurs in the case of endo-amylases, when DP of substrate exceeds the number of subsites ($n > m$) (see Fig. 2).
3) Since k_0/K_m contains the productive terms only, it is useful for determining subsite affinities by using linear substrates of different DP's (see below). Especially in the case of glucoamylase, there is only one productive binding mode (see Fig. 1), which simplifies the evaluation of subsite affinities a great deal.

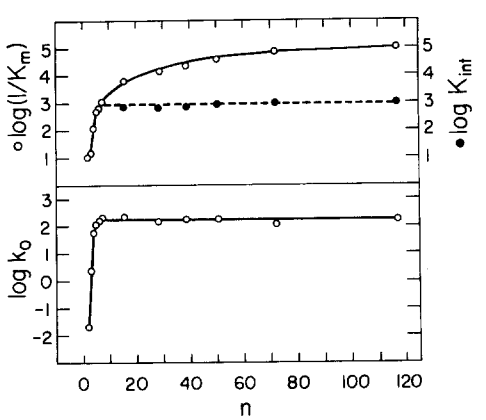

Fig. 2. Dependences of the Michaelis constant K_m and the molecular activity k_0 on the degree of polymerization n of linear substrates for Taka-amylase A-catalyzed reactions (open circles). The closed circles show the intrinsic association constant K_{int} (see Ref. 16).

Evaluation of subsite parameters A_i and k_{int}

There are two ways for evaluating subsite affinites A_i's. The first is called the 'kinetic method', originated by one of the authors (K. H.) for glucoamylase (12). As described above, the Michaelis parameters for a series of linear substrates are used to determine A_i's and k_{int}. It may be readily seen that A_i's for $i > 2$ can be obtained from the k_0/K_m values for n-mer and (n + 1)-mer substrates, successively, by using the following equation derived from Eqs. 6 and 8:

$$A_{n+1} = RT[\ln(k_0/K_m)_{n+1} - \ln(k_0/K_m)_n] \qquad (9)$$

where $n = 2, 3, 4, \ldots$ (see Fig. 1). The other three parameters A_1, A_2 and k_{int} can be determined to make the best fit for K_m and k_0 values of all the substrates. For details, the original paper (13) is to be referred to. The values of the subsite parameters, A_i's and k_{int}, are summarized in Table 1 and in Fig. 5 below. Figure 3 shows the dependence of K_m, k_0, and k_0/K_m (the rate parameters) on DP of linear substrates, in which the solid lines are the theoretical curves calculated according to Eqs. 4–6 and 8 by using the subsite parameters (A_i and k_{int}) obtained from the experimental values of K_m and k_0 (open circles). The good agreement between theory and experiment strongly supports the validity of the subsite theory.

Another important method for evaluating subsite affinities is 'the product analysis method' developed by Thoma et al. (22, 23) and by Suganuma et al. (24). This method is based on the quantitative analysis of reducing end-labeled products produced from a series of reducing end-labeled maltooligosaccharides. As seen from Fig. 4, the ratio of the rate of the formation of end-labeled glucose (v_I) to that of maltose (v_{II}), which is proportional to the ratio of $K_{n,p}$'s for the two productive binding

Table 1. Values of subsite affinities A_i's and intrinsic rate constant of hydrolysis k_{int} for *Rhizopus delemar* glucoamylase at pH 4.5, 25 °C (12–14).

Subsite (i)*	1	2	3	4	5	6	7
Subsite affinity (A_i) (kcal/mol)	0	4.85	1.59	0.43	0.22	0.11	0.10
k_{int} (s^{-1})	77						

* The subsites are numbered from the nonreducing end side. The catalytic site is situated between Subsites 1 and 2.

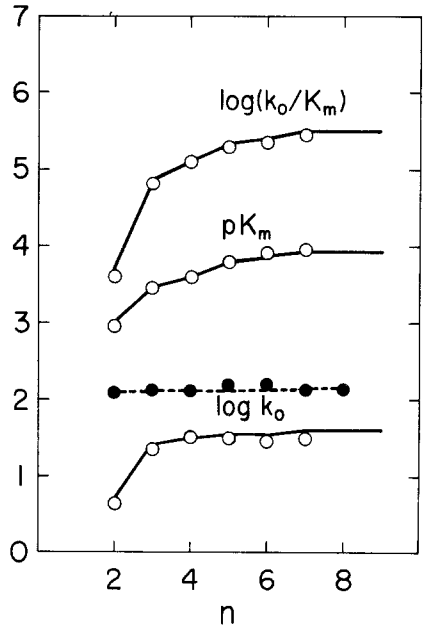

Fig. 3. Dependences of the Michaelis constant K_m (in M unit), the molecular activity k_0 (s^{-1}) and their ratio k_0/K_m on the degree of polymerization n of the substrates for glucoamylase-catalyzed reaction (open circles) observed at pH 4.5, and 25 °C. The solid lines are the theoretical ones calculated according to Eqs. 4 ~ 6 and 8 by using the values of the subsite affinities (A_i's) and the intrinsic rate constant (k_{int}) listed in Table 1. Closed circles and broken line show the observed and the theoretical values of k_0 for the α-glucosidase catalyzed reaction, respectively (pH 5.0, 37 °C) (26).

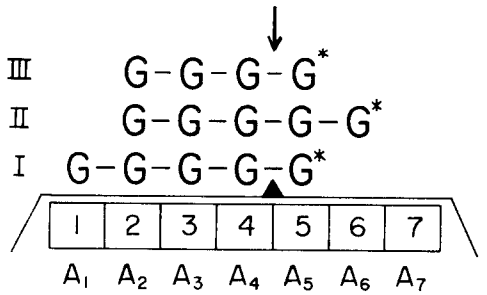

Fig. 4. Schematic model for the productive binding modes of maltopentaose (I and II) and maltotetraose (III) on an endoamylase. G and G* represent unlabeled and labeled glucose residue of the substrate, respectively. The wedge indicates the catalytic site, and the arrow shows the position at which the substrate linkages are cleaved. The boxes indicate the subsites which are numbered from the nonreducing end side, and A_i denotes the subsite affinity of the i-th subsite.

modes (I and II) of the original substrate, maltopentaose in this case (n = 5, j = 1 and 2). Hence we have, from Eq. 8

$$v_I/v_{II} = K_{5,1}/K_{5,2} = \frac{\exp[(A_1 + A_2 + A_3 + A_4 + A_5)/RT]}{\exp[(A_2 + A_3 + A_4 + A_5 + A_6)/RT]} = \exp[(A_1 - A_6)/RT] \quad (10)$$

Thus the relative values of A_i's except for those of the two 'essential' subsites (the subsites on both sides of the catalytic site) can be obtained (22, 23). This method cannot be applied to exo-amylase (e.g., glucoamylase) for which only one productive binding mode can exist.

Suganuma et al. (24) deviced a more sophisticated method which can overcome this deficiency: if a set of two end-labeled maltooligosaccharides differing in DP by one are used, we can directly evaluate the subsite affinity of the subsite which is not occupied by the shorter substrate but is occupied by the longer one (see Fig. 4), from the ratio of the rates of formation of the two end-labeled products (v_{II}/v_{III}). For example, in the case of Fig. 4, we have

$$v_{II}/v_{III} = \exp(A_6/RT) \quad (11)$$

where v_{II} and v_{III} are the rates of formation of end-labeled maltose and glucose from the binding modes II and III, respectively.

Generally speaking, the kinetic method is best suited for exo-amylases, especially for glucoamylase, although it is applicable to endo-amylases for which the location of the catalytic site is known. On the other hand, the product analysis method is useful for endo-amylases usually, which enables us to determine the location of the catalytic site too (22, 23), but the A_i values of the two 'essential subsites' cannot be determined, since they must be occupied always in any productive complex. Thus the kinetic method must be used supplementarily. By using these two methods, we can determine all the subsite parameters, A_i's and k_{int}, for every amylase. Figure 5 shows the result obtained for several amylases and an α-glucosidase (buckwheat) in histograms. The negative or near zero value of A_i at one of the essential subsites is rather commonly seen in most of the enzymes studied, which suggests most probably that some distortion induced in a glucose residue (or possibly in the enzyme subsite) over-

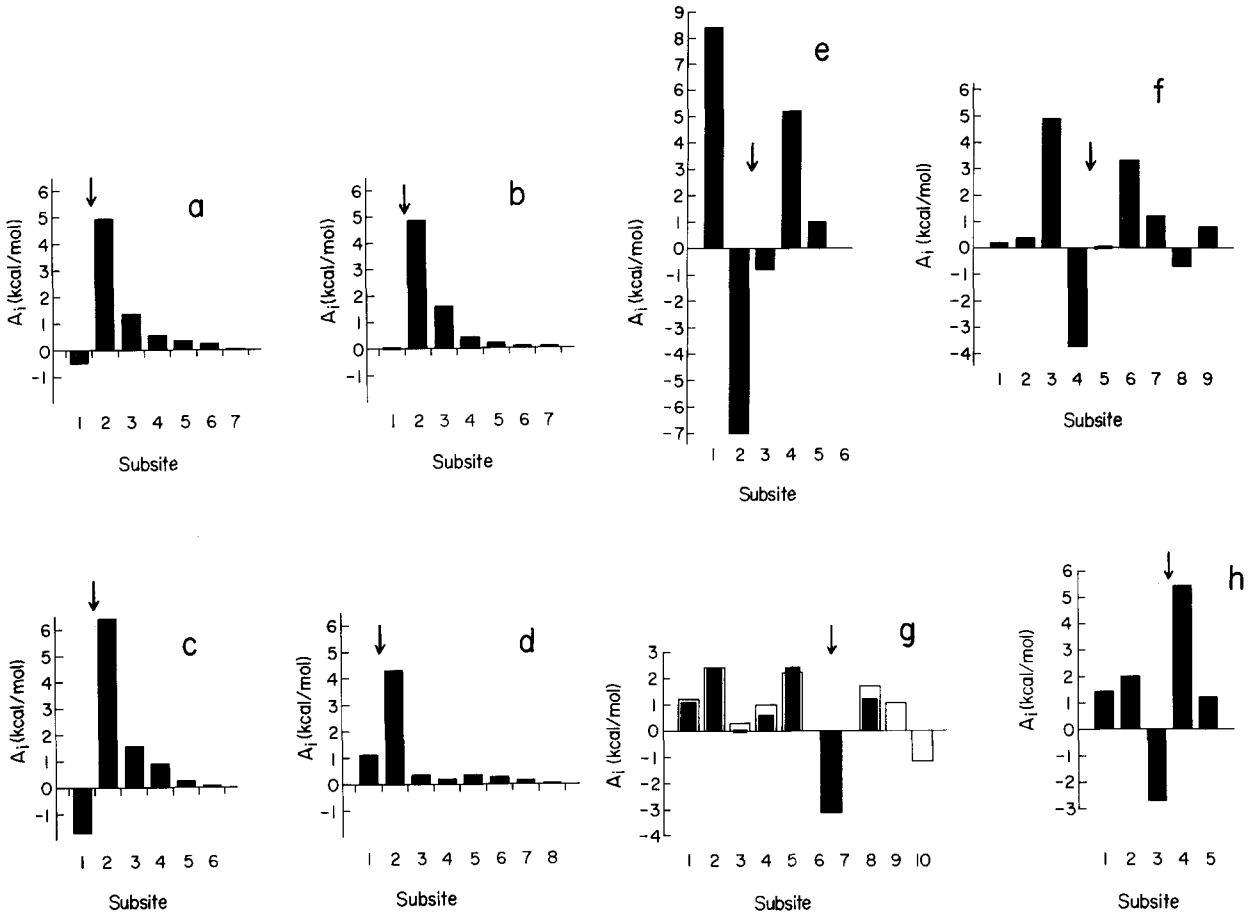

Fig. 5. Histograms showing the characteristic arrangement of subsite affinities of various amaylases and an α-glucosidase. (a) Glucoamylase from *Rh. niveus* (15). (b) Glucoamylase from *Rh. delemar* (12–14). (c) Glucoamylase from *C. resinae* (15) (calculated from the original data of Michaelis parameters in Ref. 25 for 'glucoamylase S'). (d) α-glucosidase from buckweat (26). (e) β-amylase from soybean (27, 28). (f) Taka-amylase A from *Asp. oryzae* (24). (g) Liquefying α-amylase from *B. subtilis;* the subsite affinities were obtained by the kinetic method (black pillars) (29) and the product analysis method (white pillars) (22). (h) Saccharifying α-amylase from *B. subtilis* (30). The arrows show the cleavage point.

whelms or compensates the binding affinity due to the specific and important interactions at the relevant subsite. This seems to be a common pattern for at least glycosyl hydrolases, as evidenced for lysozyme (18–21). Thus it is reasonable to assume that gluconolactone (gluconic acid-1,5-lactone) having a distorted pyranose ring structure resembling the transition state will be bound at the essential subsite with low A_i value.

Results and discussion

1. Subsite structure of glucoamylases

The subsite parameters, A_i's and k_{int}, have been determined according to the principle mentioned above for three kinds of glucoamylases, a fractionated isozyme (the major one) from *Rhizopus niveus* (15), one from *Rhizopus delemar* (12–14), and one from *Cradosporium resinae* (calculated by Tanaka et al. (15) from the original data of Michaelis parameters obtained by Lineback (25) for 'glucoamylase S'). The subsite affinities of these glucoamylases are shown in Fig. 5 (a ~ c) together with the

ones determined by Chiba et al. (26) for buckweat α-glucosidase (d)*.

It is noteworthy that there is a common feature in their subsite structures; Subsite 1 has a small negative or near zero A_i value, lower than that of Subsite 3, and Subsite 2 has the largest positive affinity. Subsites 4 ~ 7 are of rather minor importance. The negative or near zero value of the first subsite affinity A_1 suggests distortion of pyranose ring of the nonreducing end glucose residue of a substrate bound in a productive mode. The difference in the relative magnitudes between A_i's of Subsites 1 and 3 for glucoamylases and buckwheat α-glucosidase is clearly reflected on their difference in their action pattern, i.e., the DP dependence of the molecular activity k_0 (or the rate of hydrolysis at high substrate concentration), as seen from Fig. 3.

2. To which subsite does gluconolactone bind?

As was mentioned earlier, gluconolactone may be regarded as a transition state analogue for glucoamylase as well as for lysozyme, and is expected to bind to Subsite 1, one of the essential subsites. In this section, the investigation of the subsite to which gluconolactone binds will be described. Several lines of evidence have strongly suggested that gluconolactone binds at Subsite 1, as was expected.

a) Steady-state inhibition kinetic studies (32)

The subsite structure of glucoamylase (Fig. 5a ~ c) indicates that there are only one productive (j = 1) and predominantly only one nonproductive binding mode (j = 2) to be considered for every linear substrate. (For the nonproductive binding of an n-mer substrate, $K_{n,2}/K_{n,3} = \exp[(A_2 - A_3)/RT] = 240 \sim 2\,800$ for the glucoamylases). This simplifies kinetic treatments very much. For example, $\sum_p K_{n,p}$ and $\sum_q K_{n,q}$ reduce to $K_{n,1}$ and $K_{n,2}$, respectively, in Eqs. 4 ~ 6.

An inhibitor which binds only to Subsite 1 (designated by I_1) will inhibit the productive binding but not the nonproductive one (see Fig. 6), while the one which binds to Subsite 2 (designated by I_2) will inhibit both the productive and the nonproductive bindings. Thus the steady-state rate equations for the inhibition of the two types of inhibitors must be different in form: in both cases, the rate equation takes the same form:

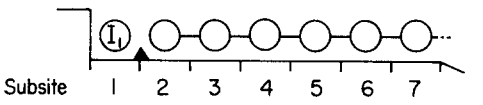

Fig. 6. Schematic representation of the ternary complex EIS_q. Open circles show the glucose residues of a substrate, and I_1 represents the inhibitor which is bound at Subsite 1.

$$v = V_a s/(K_a + s) \tag{12}$$

where s is the substrate concentration, V_a and K_a are the apparent maximum velocity and the apparent Michaelis constant in the presence of an inhibitor I, irrespective of the type of inhibition. However, the physical meanings of V_a and K_a are different depending on whether I inhibits both the productive and the nonproductive binding or only the nonproductive binding.

In the former case, where I is bound at Subsite 2, we have

$$K_a = K_m(1 + i/K_{i_2}) \tag{13}$$

$$V_a = V \tag{14}$$

where K_m and V are the Michaelis constant and the maximum velocity in the absence of the inhibitor I, i represents the inhibitor concentration $[I]_0$, and K_{i_2} is the inhibitor constant, or the dissociation constant of EI complex in which I is bound at Subsite 2 in this case.

In contrast, in the latter case where I binds to Subsite 1 inhibiting the nonproductive binding of a substrate only, we have

$$K_a = \frac{K_m(1 + i/K_{i_1})}{1 + (K_m/K_s')(i/K_{i_1})} \tag{15}$$

$$V_a = \frac{V}{1 + (K_m/K_s')(i/K_{i_1})} \tag{16}$$

where K_s' is the dissociation constant of the substrate S from the ternary complex EIS_q, where I is bound at Subsite 1 and S covers Subsites 2, 3, ..., bound in the nonproductive mode (see Fig. 6), and K_{i_1} is the dissociation constant of EI in which I is bound at Subsite 1.

* The critical difference between glucoamylase and α-glucosidase resides in their reaction mechanisms: glucoamylase produces β-glucose, whereas α-glucosidase produces α-glucose (31).

It is now apparent that the former case corresponds to the competitive inhibition, whereas the latter to the mixed type inhibition defined by Dixon and Webb (33). As seen from Fig. 7A, phenyl α-glucoside, for which the glucose residue is expected to be bound at Subsite 2 having the largest A_i, actually exhibits the purely competitive inhibition (32), as expected from the above argument. The same is true for the inhibition by glucose (34). On the other hand, gluconolactone was found to show a mixed type inhibition (Fig. 7B), in which two straight lines in the double reciprocal plot intersect at a point in the third quadrant (see Eqs. 15 and 16; the K_i value of gluconolactone obtained was 1.5 mM (32)). This result gives a good evidence for the binding of gluconolactone at Subsite 1.

b) Difference absorption spectrophotometry (35)

One of the authors (M. O.) found, by the difference absorption spectrophotometry, that a characteristic trough around 300 nm appears when maltose and amylose are bound to glucoamylase, as seen from Fig. 8A (35). A similar trough is seen upon the binding of gluconolactone with the enzyme (35). Interestingly, glucose and isomaltose do not show this characteristic trough (Fig. 8B) (35, 36). From the study with tryptophan and its derivatives (37) as model compounds, the origin of the trough was considered to reflect a change in the electrostatic environment of a tryptophan residue (abbreviated by Trp) of glucoamylase; the distance between the Trp and some positive or negative charge of a certain amino acid residue of the enzyme is supposed to be decreased or increased upon the binding of the linear substrates or gluconolactone, respectively (35). Since Subsite 1 is occupied by every linear substrate and gluconolactone but not by glucose, it is quite reasonable to consider that the relevant Trp responsible for the trough is located in Subsite 1, adjacent to the catalytic site. From the pH dependence of the rate parameters for glucoamylase-catalyzed reactions, the catatytic re-

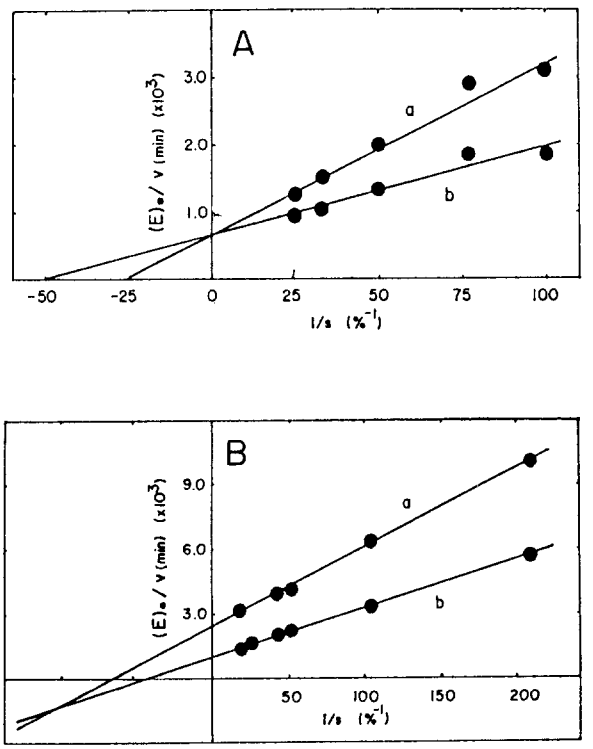

Fig. 7. Double-reciprocal plot for the inhibition by phenyl α-glucoside (A) and by gluconolactone (B) of maltodextrin hydrolysis catalyzed by glucoamylase. (A) Glucoamylase, 0.040 μM; phenyl α-glucoside, (a) 10.0 mM, (b) 0.0 mM. (B) Glucoamylase, 0.071 μM: gluconolactone, (a) 0.96 mM, (b) 0.0 mM.

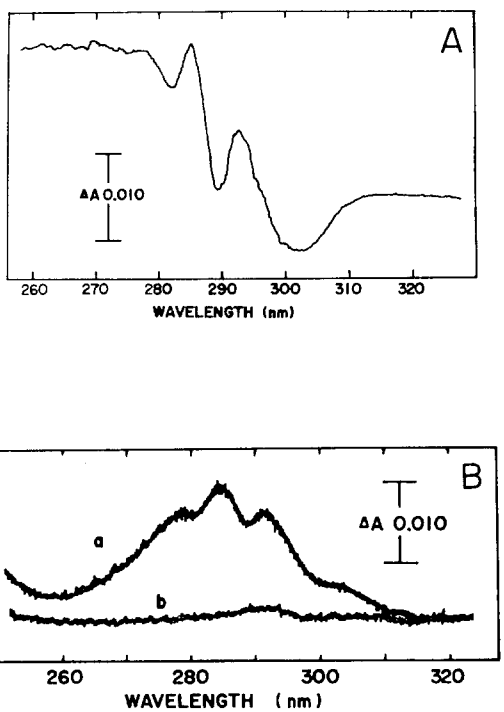

Fig. 8. The difference spectra of glucoamylase caused by the binding of maltose (A) and glucose (B). (A) Glucoamylase, 11.5 μM; maltose, 139 mM. (B) Glucoamylase, 7.7 μM; glucose, (a) 0.96 M, (b) 0 M.

sidues, i.e., the essential ionizable groups of glucoamylase, have been identified to be a carboxyl and a carboxylate group (38). It is possible, therefore, that the negative charge of the carboxylate ion could be involved in the appearance of the 300 nm trough. Since the ligands (substrates and analogues) are not charged, the binding of the ligands at Subsite 1 could induce some conformational change in its vicinity so that the negative charge becomes further to the tryptophan residue.

c) Fluorometric titration of the enzyme with gluconolactone in the presence of glucose

If gluconolactone binds to Subsite 1 and glucose to Subsite 2, the binding of glucose and gluconolactone with the enzyme would not be competitive but noncompetitive, and a ternary complex, gluconolactone–glucose–enzyme, could be formed in the coexistence of the two ligands. The protein fluorescence of the enzyme arising from tryptophan residue(s) has been known to be partially quenched by the binding of glucose as well as gluconolactone and linear substrates (39, 40). Thus the fluorometric titration of the enzyme with gluconolactone in the presence and absence of glucose is considered useful for confirming the above-mentioned binding modes of the ligands. Figure 9 shows a typical example of the results obtained from the fluorometric titration of the enzyme with gluconolactone in the presence of glucose or glucosides. Obviously the experimental points do not fit the theoretical curve for competitive binding of gluconolactone and glucose or some glucosides (curve A), but can be fitted to the theoretical curve based on a noncompetitive binding mechanism with a weak positive cooperativity between the two binding sites for gluconolactone and glucose or glucosides (curve B). The relevant expression for the percentage of the fluorescence decrease, ΔF, as functions of the concentrations of the ligands, gluconolactone (L) and glucose or glucosides (methyl α-glucoside and phenyl β-glucoside) (G), is as follows (41):

$$\Delta F = \frac{\Delta F^{G}_{max}[G]_0/K_G + \Delta F^{L}_{max}[L]_0 + \Delta F^{GL}_{max}[L]_0[G]_0/(K_G K'_L)}{1 + [G]_0/K_G + [L]_0/K_L + [L]_0[G]_0/(K_G K'_L)} \quad (17)$$

where K_G and ΔF^{G}_{max} are the dissociation constants of glucose or glucoside in the binary EG complex and the maximum percentage of fluorescence decrease in the EG complex, respectively, K_L and ΔF^{L}_{max} are those values for gluconolactone in the binary EL complex, K'_L and ΔF^{GL}_{max} are the dissociation constants of gluconolactone from the ternary complex ELG and the maximum percentage of fluorescence decrease in the ELG complex, respectively. The concentration terms in the square brackets with the subscript zero are the initial concentrations of the ligands, L and G. The values of K's and ΔF_{max}'s for glucose or glucosides and gluconolactone are determined from the separate experiments with the individual analogues, and by using these values K'_L and ΔF^{GL}_{max} can be determined to have the best fit to the experimental points according to Eq. 17. The values of the constants thus obtained are summarized in Table 2. The fact that ΔF^{GL}_{max} is nearly equal to ΔF^{L}_{max} indicates that the fluorescence of only one Trp is quenched upon binding of either gluconolactone or glucose (and glucosides). Moreover, it is obvious from Table 2 that gluconolactone is bound at Subsite 1 and not Subsite 2, since there is no steric hindrance (resulting in possible competition between gluconolactone and glucosides) due to aglycon moiety of glucosides, which would disturb or prohibit the binding of gluconolactone at Subsite 2, if glucose and gluc-

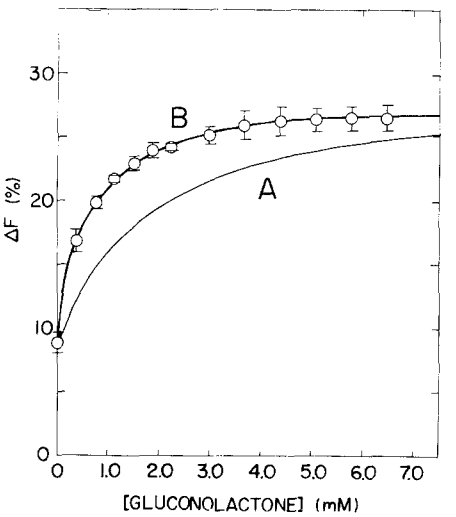

Fig. 9. Dependence of ΔF on the initial concentration of gluconolactone in the presence of 100 mM glucose (open circles). Glucoamylase; 0.9 μM. pH 4.5, 10 °C; excitation wavelength λ_{ex} = 280 nm. The solid curve A represents a theoretical curve for the competitive type binding of gluconolactone and glucose. The solid line B is obtained for the noncompetitive type binding according to Eq. 17 using the values listed in Table 2.

Table 2a. Dissociation constant (K_d) and percentage of maximum fluorescence intensity decrease (ΔF_{max}) of the enzyme-ligand complex (pH 4.5, 10 °C).

Ligand	λ_{ex} (nm)*	K_d (mM)	ΔF_{max} (%)
gluconolactone	280	1.08 ± 0.04	30.1 ± 0.3
gluconolactone	295	1.09 ± 0.09	32.0 ± 1.0
glucose	280	127 ± 9	20.0 ± 0.6
methyl α-glucoside	280	540 ± 60	24.1 ± 1.5
phenyl β-glucoside	295	10.9 ± 0.5	18.4 ± 0.3

* λ_{ex} shows the excitation wavelength.

Table 2b. Dissociation constants of gluconolactone (K'_L) and glucose or glucosides (K'_G) from the ternary enzyme-gluconolactone-glucose (or -glucoside) complex and the percentage of maximum fluorescence intensity decrease of the ternary complex (ΔF^{GL}_{max}) obtained from the fluorometric titration with gluconolactone in the presence of glucose or glucosides (pH 4.5, 10 °C).

Glucose or glucoside	λ_{ex} (nm)*	K'_L (mM)	K'_G (mM)	ΔF_{max} (%)
glucose	280	0.49 ± 0.14	58 ± 20	29 ± 1
methyl α-glucoside	280	0.30	150	31
phenyl β-glucoside	295	0.41	4.1	28

* λ_{ex} shows the excitation wavelength.

osides were bound at Subsite 1 and gluconolactone at Subsite 2. The results described in this section, together with those in the preceding sections, confirmed that the transition state analogue gluconolactone binds to Subsite 1 and unstrained glucopyranose residue binds to Subsite 2.

3. Stopped-flow kinetic studies on ligand binding

Based on the results obtained from the equilibrium studies and the steady-state kinetic studies on the interaction between glucoamylase and linear substrates and analogues, the stopped-flow kinetic studies were done directly on the ligand binding with the enzyme. The decrease in the enzyme fluorescence intensity was used mainly for monitoring the fast reactions concerned, although some kinetic study on glucoamylase-maltotriose interaction has been made by using the 300 nm trough as the probe (42). The results of the fluorescence stopped-flow studies will be summarized below. As for details, the original papers are to be referred to (43, 44).

a) Binding of maltose and gluconolactone (43)

As a simplest substrate, maltose was chosen for the study of binding kinetics. Glucose, a competitive inhibitor as well as the essential constituent unit of substrates, was found to bind with the enzyme too fast to be measured with the stopped-flow technique (the half-time at 5 °C is shorter than about 0.2 ms). Gluconolactone was therefore chosen as a nonsubstrate specific ligand for this enzyme.

Two typical examples of the fluorescence stopped-flow traces for the binding of the two ligands are shown in Fig. 10. In both cases, only one relaxation was observed. The apparent first order rate constant k_{app}, or the reciprocal relaxation time $1/\tau$ (45), obtained from the time courses showed hyperbolic dependence on the ligand concentra-

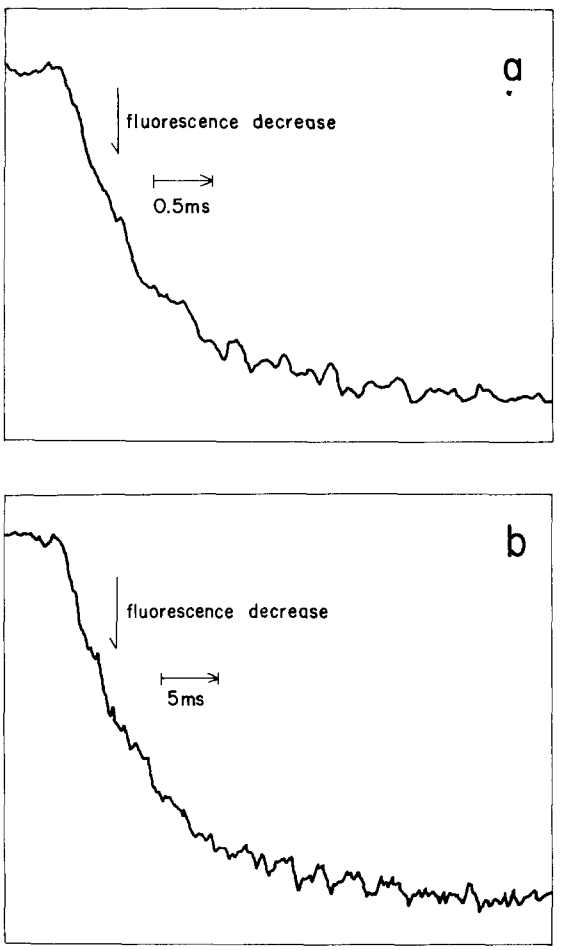

Fig. 10. Typical time course of the fluorescence intensity decrease caused by the binding of maltose (a) and gluconolactone (b) to glucoamylase. Excitation wavelength λ_{ex} = 280 nm; 9 times accumulation. (a) Glucoamylase, 13.1 μM; maltose, 15 mM. pH 4.5, 5 °C. (b) Glucoamylase, 6.1 μM; gluconolactone, 7.5 mM. pH 4.5, 10 °C. (Concentrations refer to those in the reaction mixture.)

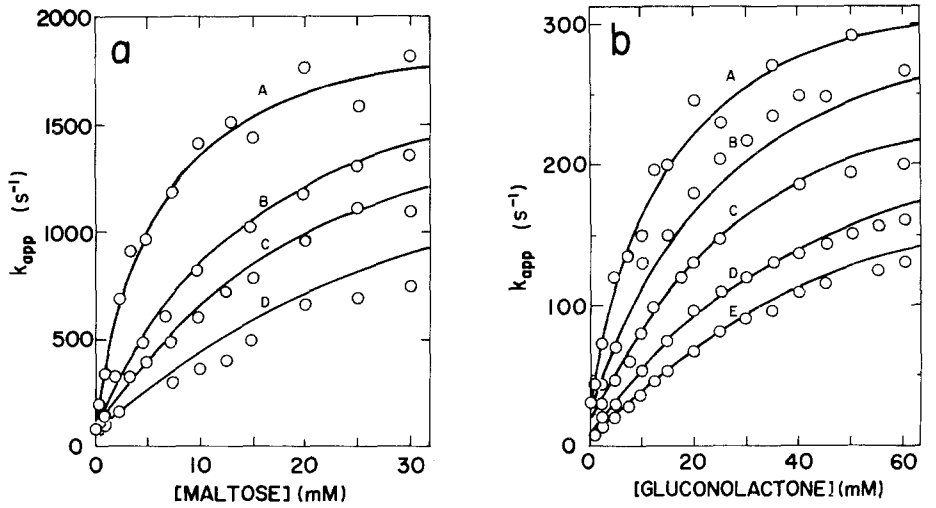

Fig. 11. Dependence of k_{app} on the initial concentrations of maltose (a) and gluconolactone (b) in the absence and presence of glucose. (a) Glucoamylase, 13.1 μM; glucose, 0 (A), 50 (B), 100 (C), and 200 mM (D) at pH 4.5, 5 °C. (b) Glucoamylase, 6.1 μM; glucose, 0 (A), 50 (B), 100 (C), 200 (C), and 250 mM (D) at pH 4.5, 10 °C. The solid lines are the theoretical curves (see text).

tion, as seen from curves A of Fig. 11a and b. As the basic theory of relaxation kinetics (45) tells, this concentration dependence indicates that the binding is not a single step but most probably occurs in a two-step mechanism, in which a slow unimolecular process (often called the 'isomerization') follows a fast bimolecular binding process:

$$E + L \underset{k_{-1}}{\overset{k_{+1}}{\rightleftharpoons}} EL \underset{k_{-2}}{\overset{k_{+2}}{\rightleftharpoons}} EL^* \qquad (18)$$

fast slow

where L denotes a ligand (a substrate or an analogue), EL an intermediate (most probably a loosely bound) complex, and EL* a final (tightly bound) complex, and k's are the rate constants for the elementary steps as indicated in Eq. 18. At maximum two phases with different relaxation times (or rate constants) could be expected to be observed for this scheme (45). When the ligand exists in large excess over the enzyme, we have:

$$1/\tau_1 = k_{app_1} = k_{+1}[L]_0 + k_{-1} \qquad (19)$$

$$1/\tau_2 = k_{app_2} = \frac{k_{+2}[L]_0}{K_{-1} + [L]_0} + k_{-2} \qquad (20)$$

where k_{app_1} ($= 1/\tau_1$) and k_{app_2} ($= 1/\tau_2$) are the apparent first order rate constants of the faster and slower phases, respectively, $[L]_0$ is the initial concentration of a ligand, and K_{-1} ($= k_{-1}/k_{+1}$) is the dissociation constant of the intermediate complex EL. For a single step binding mechanism, $E + L \rightleftharpoons EL$, Eq. 19 is valid, and k_{app} will show linear dependence on $[L]_0$. If only one relaxation is observed and k_{app} shows hyperbolic concentration dependence as Eq. 20, the most reasonable interpretation is that we are observing the slower one of the two possible relaxations, the faster one being missed from the observation. (Either when the faster process has no observable signal change or it is essentially too fast to be observed by the technique employed, the fast bimolecular process cannot be observed actually.) In this case, we can evaluate K_{-1}, k_{+2} and k_{-2}, from the plot of k_{app} against $[L]_0$, although individual values of k_{+1} and k_{-1} cannot be known.

The values of these three kinetic parameters obtained from curves A of Fig. 11 for the two ligands are summarized in Table 3. Another important

Table 3. Kinetic parameters for the binding of maltose and gluconolactone to glucoamylase (pH 4.5).

Ligand	Temperature	K_{-1} (mM)	$k_{+2}(s^{-1})$	$k_{-2}(s^{-1})$
maltose	5 °C	5.61	2 030	45.1
gluconolactone	10 °C	14.3	348	22.2

finding is that the fluorescence change is occurring solely in the slower unimolecular process, no fluorescence change being involved in the faster bimolecular process (43). This conclusion is obtainable from the comparison between the percentage of fluorescence signal change observed in the stopped-flow method and that of the static one (the total change) before and after the binding reaction.

Effect of glucose on the binding kinetics of gluconolactone and maltose: as was mentioned above, it is supposed that glucose binds to Subsite 2, whereas both gluconolactone and maltose occupy Subsite 1. If this is the case, the competition for the binding will be expected to occur between glucose and maltose, but not between glucose and gluconolactone. It is interesting to see, therefore, how glucose affects the binding kinetics of maltose and gluconolactone differently.

The results are shown in Figs. 11 and 12. As was expected, glucose inhibits the rate processes of the binding of either maltose or gluconolactone (Fig. 11), but a critical difference in its effect on maltose and gluconolactone resides in that glucose slows down the k_{-2} process for gluconolactone binding, but does not affect that for maltose binding (Fig. 12a-iii and b-iii). Based on these results, we proposed the mechanism of binding for the two ligands, maltose and gluconolactone, as shown in Fig. 13. According to this mechanism, it is apparent that glucose, which is bound at Subsite 2, will inhibit the formation of EL and EM, the loosely bound intermediate complexes, resulting in slowing down the overall binding rate processes for both ligands. However, since glucose can bind to EL* but not to

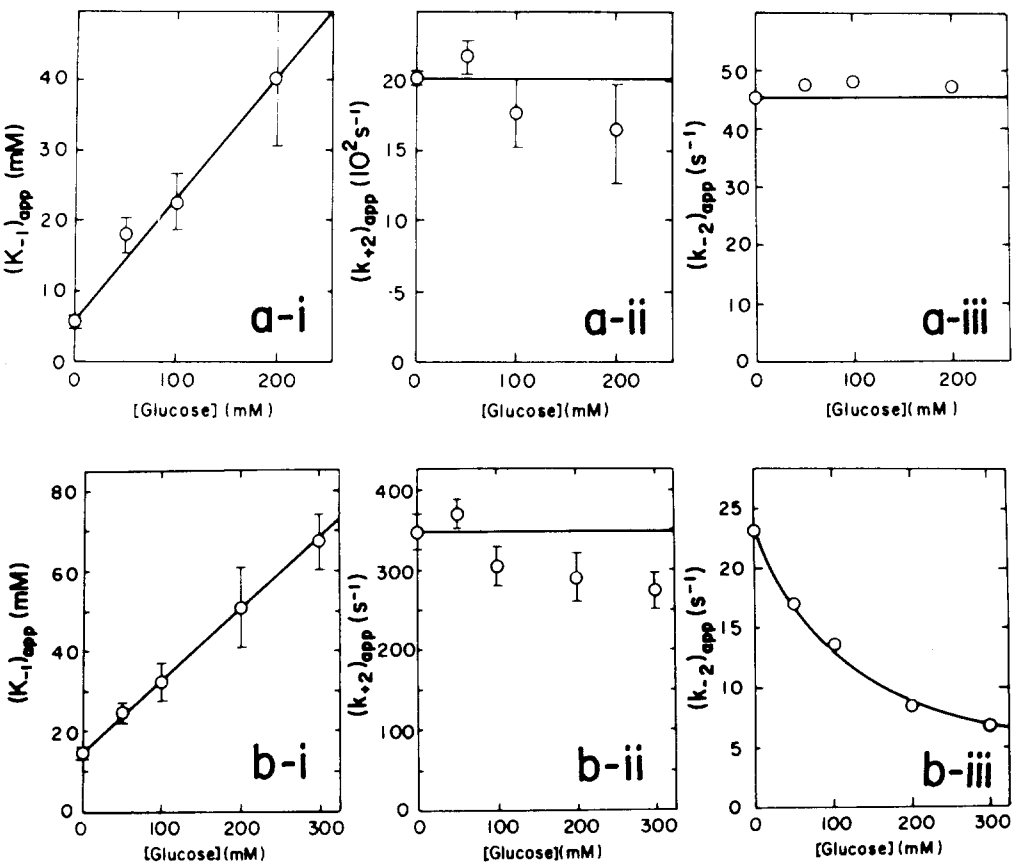

Fig. 12. Effect of glucose concentration on the kinetic parameters for the binding of maltose (a) and gluconolactone (b). $(K_{-1})_{app}$, $(k_{+2})_{app}$, and $(k_{-2})_{app}$ are the apparent values of K_{-1}, k_{+2}, and k_{-2} in the presence of glucose. The solid lines were drawn according to the following equations: $(K_{-1})_{app} = \{1 + ([G]_0/K_G)\}$ (a-i and b-i), $(k_{-2})_{app} = k_{+2}$ (a-ii and b-ii), $(k_{-2})_{app} = k_{-2}$ (a-iii), and $(k_{-2})_{app} = k_{-2}/\{1 + ([G]_0/K'_G)\}$ (b-iii), using K_{-1} 5.61 mM, $K_G = 35$ mM, $k_{+2} = 2\,030\ s^{-1}$, and $k_{-2} = 45.1\ s^{-1}$ (a-i ~ iii) and $K_{-1} = 14.3$ mM, $K_G = 81.1$ mM, $K'_G = 120$ mM, $k_{+2} = 348\ s^{-1}$, and $k_{-2} = 22.2\ s^{-1}$ (b-i ~ iii) (cf. Eqs. 20, 22, and 24).

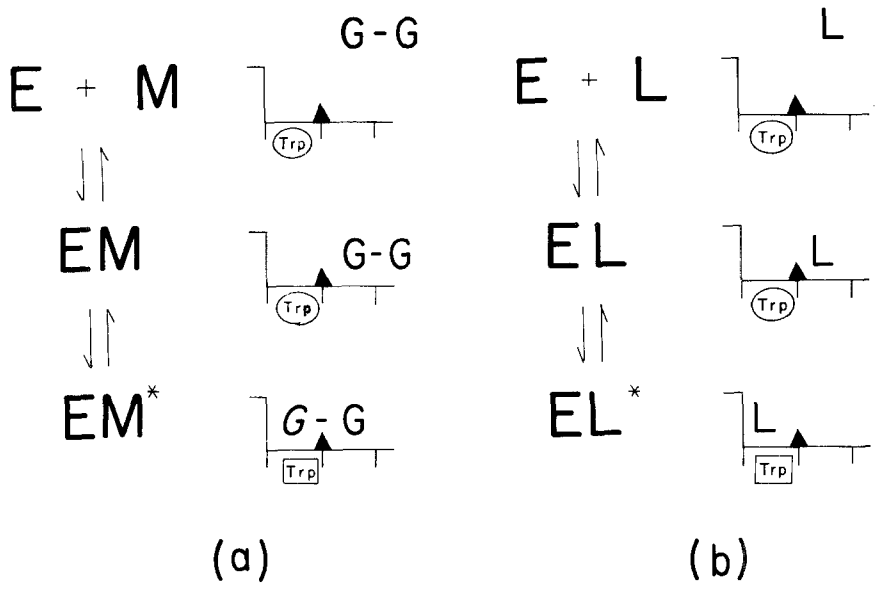

Fig. 13. Proposed mechanism of the binding processes of maltose (a) and gluconolactone (b). (Trp) and [Trp] indicate the emissive and the quenched states of the tryptophan fluorescence, respectively.

EM*, the tightly bound complexes, a ternary complex ELG* can exist for gluconolactone, whereas no EGM* complex can exist for maltose. This explains why glucose affects the k_{-2} process for gluconolactone (the shift of L from Subsite 1 to Subsite 2 which is occupied by G) and not for maltose. The reaction schemes and the apparent rate constant k_{app} in the presence of glucose are as follows (43):
For maltose (M):

$$\begin{array}{ccccc} E + M & \underset{k_{-1}}{\overset{k_{+1}}{\rightleftharpoons}} & EM & \underset{k_{-2}}{\overset{k_{+2}}{\rightleftharpoons}} & EM^* \\ + & & & & \\ G & & & & \\ \Big\downarrow\Big\uparrow\ K_G & & & & \\ EG & & & & \end{array} \qquad (21)$$

$$k_{app} = \frac{k_{+2}[M]_0}{K_{-1}\{1 + ([G]_0/K_G)\} + [M]_0} + k_{-2} \qquad (22)$$

For gluconolactone (L):

$$\begin{array}{ccccc} E + L & \underset{k_{-1}}{\overset{k_{+1}}{\rightleftharpoons}} & EL & \underset{k_{-2}}{\overset{k_{+2}}{\rightleftharpoons}} & EL^* \\ + & & & & + \\ G & & & & G \\ \Big\downarrow\Big\uparrow\ K_G & & & & \Big\downarrow\Big\uparrow\ K'_G \\ EG & & & & ELG^* \end{array} \qquad (23)$$

$$k_{app} = \frac{k_{+2}[L]_0}{K_{-1}\{1 + ([G]_0/K_G)\} + [L]_0} + \frac{k_{-2}}{1 + ([G]_0/K'_G)} \qquad (24)$$

where K_G and K'_G are the dissociation constants of glucose from the EG and ELG* complexes, respectively, and the binding of glucose with the enzyme was regarded as a rapid equilibrium.

By using the values of the kinetic parameters (Table 3) and the values of K_G and K'_G obtained from Fig. 12, theoretical curves were drawn for Fig. 11. Good agreement between the theoretical curves and the experimental points strongly supported the validity of the mechanism proposed, again confirming that gluconolactone and glucose occupy Subsite 1 and Subsite 2, respectively.

b) Effect of chain length of substrate on the equilibrium and the kinetic parameters (44)

For a series of linear substrates, DP = 2 ~ 7, the same kind of static and kinetic studies have been made. For all, the mechanism of Eq. 18 was considered valid. The results are summarized in Table 4 and Fig. 14.

The dissociation constant of the enzyme–substrate complex, K_d, obtained from the static fluorometric titration, decreases with increasing DP, as

Table 4. Values of constants obtained from the steady-state kinetics, fluorometric titration, and stopped-flow kinetics. pH 4.5, 0.5 °C.

DP	Steady-state kinetics		Fluorometric titration		Stopped-flow kinetics		
	$k_0(s^{-1})$	K_m (mM)	K_d (mM)	ΔF_{max} (%)	K_{-1} (mM)	$k_{+2}(s^{-1})$	$k_{-2}(s^{-1})$
2	0.60 ± 0.05	0.82 ± 0.07	0.55 ± 0.05	28.3 ± 0.6	7.28 ± 0.74	1 450 ± 55	55 ± 5
3	3.0 ± 0.2	0.35 ± 0.03	0.29 ± 0.05	26.7 ± 1.4	4.26 ± 1.01	903 ± 87	40 ± 3
4	3.5 ± 0.3	0.25 ± 0.03	0.14 ± 0.01	31.0 ± 0.8	5.48 ± 0.96	1 200 ± 94	18 ± 4
5	3.9 ± 0.2	0.19 ± 0.02	0.082 ± 0.01	31.6 ± 1.4	7.40 ± 0.79	1 400 ± 67	15 ± 2
6	3.9 ± 0.5	0.14 ± 0.03	0.10 ± 0.02	33.1 ± 1.9	7.81 ± 0.52	1 560 ± 44	10 ± 1
7	3.8 ± 0.3	0.11 ± 0.01	0.097 ± 0.007	34.4 ± 0.8	7.15 ± 1.27	1 520 ± 110	11 ± 3

The figure after ± shows the standard deviation.

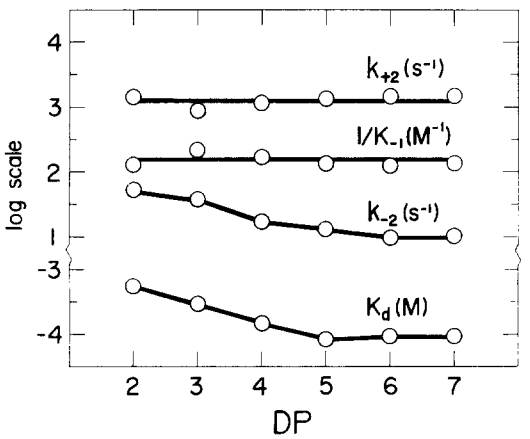

Fig. 14. Dependence of K_d, K_{-1}, k_{+2}, and k_{-2} on the degree of polymerization DP of the substrates. K_d, the dissociation constant of the enzyme-substrate complex (in M unit); $1/K_{-1}$, the reciprocal of the dissociation constant of the loosely bound intermediate complex ES_n (M^{-1}); k_{+2} and k_{-2}, the rate constant of the unimolecular process (s^{-1}) (cf. Eq. 18). pH 4.5, 0.5 °C.

well as the Michaelis constant K_m obtained from the steady-state kinetics (Table 4). Based on the two-step mechanism of Eq. 18, K_d is expressed as follows (44, 46, 47):

$$K_d = K_{-1}/\{1 + (k_{+2}/k_{-2})\} \doteqdot K_{-1}k_{-2}/k_{+2} \qquad (25)$$

since $k_{-2} \ll k_{+2}$ for all the substrates studied. It is interesting to see which kinetic parameter(s) in the two-step mechanism of Eq- 18 is affected by the substrate chain length (DP). As is obvious from Fig. 14, DP do not appreciably affect K_{-1}, k_{+2}, but k_{-2} decreases with increasing DP, in the same way as K_d.

It is noteworthy that the dissociation constant of the loosely bound intermediate complex ES_n (n = DP), K_{-1} is essentially independent of DP and that the unitary binding free energy of a substrate in this ES_n complex (the negative value of which is equal to the unitary affinity of S_n in ES_n) is quite close to the subsite affinity of Subsite 2 ($A_2 = 4.7$ kcal/mol at 0.5 °C (45)),* which is equal to the unitary binding affinity of a glucose residue to this subsite. This suggests that only one subsite, most probably Subsite 2, is occupied in this loosely bound ES_n complex. Moreover, it was confirmed for every substrate that the fluorescence change occurs solely in the unimolecular process in Eq. 18, as was found for all the ligands studied. Thus the k_{+2} step, the forward process of the unimolecular isomerization step, is most reasonably considered to be a relocation or sliding of a substrate molecule to form a productive complex, in which the nonreducing end glucose residue becomes bound at Subsite 1 (Fig. 15). The fact that the fluorescence change occurs at

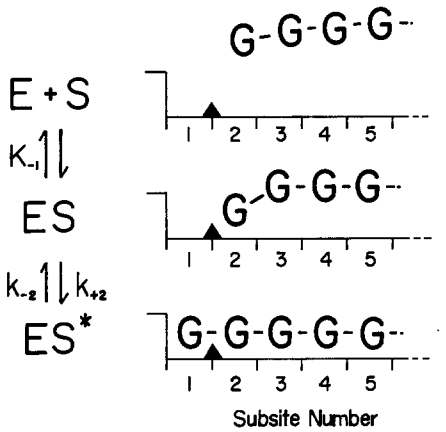

Fig. 15. Schematic representation of the proposed binding mechanism of maltooligosaccharides to the enzyme.

* This unitary binding affinity B_n is calculated as $B_n = RT \ln K_{-1} + 2.2$ kcal/mol (at 0.5 °C) = 4.9 kcal/mol.

this step indicates that a tryptophan residue situated at or quite near to subsite 1 may change its microenvironment leading to fluorescence quenching by this relocation of a substrate or a ligand.

The tightly bound ES_n^* complex is most likely the productive complex in which the glucoside bond cleavage will occur in the subsequent process. And the relocation may be related with the multiple attack mechanisms (48, 49), indicated from the comparison between the theoretical calculation and the experimentally obtained product distribution during the course of glucoamylase-catalyzed hydrolysis of amylose (4).

The similar behavior found between K_m and K_d of linear substrates (Table 4 and Fig. 14) would be naturally expected, as far as K_m can approximately be regarded as the dissociation constant of the enzyme–substrate complex.

4. Stopped-flow kinetic studies on chemical modification of tryptophan residues

Although a tryptophan residue in an enzyme protein is unlikely to be involved in the catalytic process in the enzyme reaction, it is often noticed that the chemical modification of tryptophan residue(s) leads to considerable loss of the enzyme activity (6, 50–52). Ohnishi et al. (54) found that when two of the four in total modifiable tryptophan residues of glucoamylase are oxidized by N-bromosuccinimide (NBS), its enzyme activity is lost, and also the characteristic trough near 300 nm in the difference absorption spectrum caused by the binding of maltose is diminished (8).

On the other hand, the study of the effect of solvent on the difference spectra of glucoamylase at UV region (solvent perturbation method) showed that there are four tryptophan residues accessible for ethylene glycol and two residues for polyethylene glycol (35). This suggests that two of four tryptophan residues are located on the surface of the enzyme, and the other two are situated in some cleft(s) into which ethylene glycol can enter but polyethylene glycol cannot.

The results obtained from the two different lines of approach strongly suggest that two out of four 'exposed' tryptophan residues (the total number of Trp of the enzyme is ten) may be located in the active center cleft of this enzyme.

By using fast chemical modification by NBS with the stopped-flow kinetic method, we were successful in differentiating one most reactive tryptophan residue of lysozyme (Trp 62) from four other less reactive ones, and in confirming that it is located in the active center cleft, from the protection by substrates and analogues (53). Thus we attempted to apply the same technique to glucoamylase for discriminating and locating the two less reactive and presumably partly buried tryptophan residues mentioned above.

The time course of the NBS modification of Trp residues of glucoamylase was followed by the stopped-flow method, observing the absorbance change at 280 nm and the fluorescence decrease caused by the modification (54, 55). The absorbance change tells the number of modified residues during the modification reaction, and the fluorescence change was useful for evaluating the individual rate constants of the modification for the four Trp residues.

First, the four Trp's were found to be classified into two groups, showing fast and slow phases (Fig. 16). Further analysis of the two phases revealed that each phase includes two Trp's of distinguishable rate constants. Thus all the four Trp's have been discriminated, termed $Trp^1 \sim Trp^4$, whose rate constants of modification are summarized in Table 5. Next, by examining the protection of modification in the presence of maltose, only the third-reactive Trp (Trp^3) was found to be protected by the substrate maltose. Now it is reasonable to conclude that this residue is situated in the active site, most

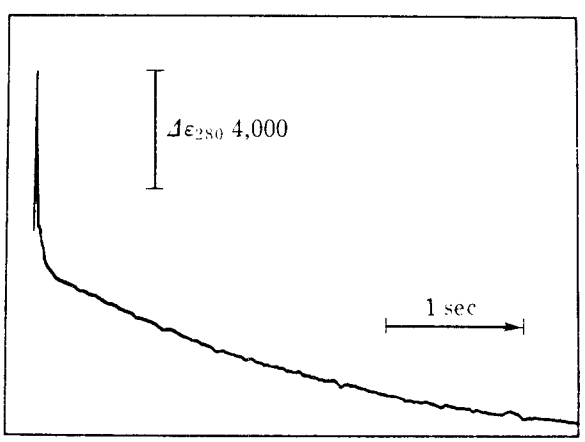

Fig. 16. A typical example of NBS modification time courses for glucoamylase observed by the absorption stopped-flow method.

Table 5. Rate constants of NBS modification for tryptophan residues of glucoamylase (pH 4.5, 25 °C).

Phase	Trp	Rate constant (M^{-1} s^{-1})
Fast	Trp^1	3.4×10^5
	Trp^2	8.8×10^4
Slow	Trp^3	2.8×10^3
	Trp^4	7.4×10^2

probably at Subsite 1, judging from the results mentioned in above sections.

Moreover, we were successful in preparing a 'selectively modified glucoamylase' in which two fast reacting Trp's are modified by NBS preferentially, by using the rapid quenching technique and gel filtration (54, 55). This preparation retained about 80% of the enzyme activity, and when mixed with NBS solution in the stopped-flow apparatus, it showed a reaction curve in which the faster phase has disappeared, leaving two slowly reacting Trp's intact. Further studies are being done with this 'selectively modified' enzyme preparation.

Concluding remarks

Because of its simple action pattern, glucoamylase was the first object of the application of the subsite theory as well as the transient kinetic studies to amylases. Several lines of evidence strongly suggested that a tryptophan residue responsible for the enzymatic action of glucoamylase is located at Subsite 1, whose fluorescence is quenched by ligand binding at this subsite, which occurs at the second step (relocation of the ligand) preceded by a rapid bimolecular binding step between the enzyme and the ligand to form a loosely bound complex.

More detailed information on the interaction between the enzyme and a ligand would be obtained in further studies, in which static and kinetic studies by using other kind of probes for monitoring and NMR techniques. The subsite theory should be extended to include branched substrates too. These subjects will be undertaken in the near future.

Finally, we would like to emphasize the importance and the usefulness of the subsite theory for amylases, to explore the structure of active site in terms of subsite, and relate it to their 'function'.

References

1. Schechter, I. and Berger, A., 1967. Biochem. Biophys. Res. Commun. 27: 157–162.
2. Morihara, K. and Oka, T., 1968. Biochem. Biophys. Res. Commun. 30: 625–630.
3. Suetsugu, N., Hirooka, E., Yasui, H., Hiromi, K. and Ono, S., 1973. J. Biochem. (Tokyo) 73: 1223–1232.
4. Kondo, H., Nakatani, H., Matsuno, R. and Hiromi, K., 1980. J. Biochem. (Tokyo) 87: 1053–1070.
5. Aoshima, H., Manabe, T., Hiromi, K. and Hatano, H., 1974. Biochim. Biophys. Acta 341: 497–504.
6. Ohnishi, M., Suganuma, T., Fujimori, H. and Hiromi, K., 1973. J. Biochem. (Tokyo) 74: 1271–1273.
7. Fujimori, H., Ohnishi, M. and Hiromi, K., 1974. J. Biochem. (Tokyo) 75: 767–777.
8. Ohnishi, M. and Hiromi, K., 1976. J. Biochem. (Tokyo) 79: 11–16.
9. Matsuura, Y., Kusunoki, M., Date, W., Harada, S., Bando, S., Tanaka, N. and Kakudo, M., 1979. J. Biochem. (Tokyo) 86: 1773–1783.
10. Matsuura, Y., Kusunoki, M., Harada, W., Tanaka, N., Iga, Y., Yasuoka, N., Toda, H., Narita, K. and Kakudo, M., 1980. J. Biochem. (Tokyo) 87: 1555–1558.
11. Tsujisaka, Y., Fukumoto, J. and Yamamoto, T., 1958. Nature 181: 770–771.
12. Hiromi, K., 1971. Biochem. Biophys. Res. Commun. 40: 1–6.
13. Hiromi, K., Nitta, Y., Numata, C. and Ono, S., 1973. Biochim. Biophys. Acta 302: 362–375.
14. Hiromi, K., 1972. In: Proteins: Structure and Function (Funatsu, M., Hiromi, K., Imahori, K., Murachi, T. and Narita, K., eds.), Vol. 2, pp. 1–46, Kodansha, Ltd., Halsted Press, Tokyo, New York.
15. Tanaka, A., Fukuchi, Y., Ohnishi, M., Hiromi, K., Aibara, S. and Morita, Y. Agric. Biol. Chem. (Tokyo) in press.
16. Nitta, Y., Mizushima, M., Hiromi, K. and Ono, S., 1971. J. Biochem. (Tokyo) 69: 567–576.
17. BeMiller, J. N., 1965. In: Starch; Chemistry and Technology (Whistler, R. L. and Paschall, E. F., eds.), Vol. 1, p. 495, Academic Press, New York.
18. Phillips, D. C., 1966. Sci. Am. 215: 78–90.
19. Phillips, D. C., 1967. Proc. Natl. Acad. Sci. U.S.A. 57: 484–495.
20. Blake, C. C. F., Johnson, L. N., Mair, G. A., North, A. C. T., Phillips, D. C. and Sarma, V. R., 1967. Proc. Roy. Soc. London B167: 378–388.
21. Chipman, D. M. and Sharon, N., 1969. Science 165: 454–465.
22. Thoma, J. A., Brothers, C. and Spradlin, J., 1970. Biochemistry 9: 1768–1775.
23. Thoma, J. A., Rao, G. V. K., Brothers, C., Spradlin, J. and Li, L. H., 1971. J. Biol. Chem. 246: 5621–5635.
24. Suganuma, T., Matsuno, R., Ohnishi, M. and Hiromi, K., 1978. J. Biochem. (Tokyo) 84: 293–316.
25. Lineback, D. R. and Baumann, W. E., 1970. Carbohydr. Res. 14: 341–353.
26. Chiba, S., Kanaya, K., Hiromi, K. and Shimomura, T., 1979. Agric. Biol. Chem. (Tokyo) 43: 237–242.
27. Kato, M., Hiromi, K. and Morita, Y., 1974. J. Biochem. (Tokyo) 75: 563–576.
28. Suganuma, T., 1974. Master's Thesis, Kyoto University.

29. Iwasa, S., Aoshima, H., Hiromi, K. and Hatano, H., 1974. J. Biochem. (Tokyo) 75: 969–978.
30. Hiromi, K., 1979. In: Developments in Food Science; Vol. 2 Food Science and Technology (Chiba, H., Fujimaki, M., Iwai, K., Mitsuda, H. and Morita, Y., eds.), Kodansha Ltd, Elsevier Scientific Publishing Company, Tokyo, Amsterdam-Oxford-New York.
31. International Union of Biochemistry (1978) Enzyme Nomenclature, pp. 276–279.
32. Ohnishi, M., Yamashita, T. and Hiromi, K., 1976. J. Biochem. (Tokyo) 79: 1007–1012.
33. Dixon, M. and Webb, E. C., 1979. Enzymes, 3rd. ed., pp. 332–381, Longman, London.
34. Hiromi, K., Kawai, M., Suetsugu, N., Nitta, Y., Hosotani, T., Nagao, A., Nakajima, T. and Ono, S., 1973. J. Biochem. (Tokyo) 74: 935–943.
35. Ohnishi, M., Kegai, H. and Hiromi, K., 1975. J. Biochem. (Tokyo) 77: 695–703.
36. Ohnishi, M., Wada, S., Yamada, T., Tanaka, A. and Hiromi, K. Denpun Kagaku (Tokyo) in press.
37. Ananthanarayanan, V. S. and Bigelow, C. C., 1969. Biochemistry 8: 3717–3723.
38. Hiromi, K., Takahashi, K., Hamauzu, Z. and Ono, S., 1966. J. Biochem. (Tokyo) 59: 469–475.
39. Hiromi, K., Ohnishi, M. and Yamashita, T., 1974. J. Biochem. (Tokyo) 76: 1365–1367.
40. Ohnishi, M., Yamashita, T. and Hiromi, K., 1977. J. Biochem. (Tokyo) 81: 99–105.
41. Hiromi, K., Tanaka, A. and Ohnishi, M., 1982. Biochemistry 21: 102–107.
42. Ohnishi, M. and Hiromi, K., 1978. Carbohydr. Res. 61: 335–344.
43. Tanaka, A., Ohnishi, M. and Hiromi, K., 1982. Biochemistry 21: 107–113.
44. Tanaka, A., Yamashita, T., Ohnishi, M. and Hiromi, K., J. Biochem. (Tokyo) (in press).
45. Eigen, M. and DeMaeyer, L., 1963. Tech. Org. Chem. 8 (Part 2): 895–1054.
46. Halford, S. E., 1975. Biochem. J. 149: 411–422.
47. Hiromi, K., 1979. Kinetics of Fast Enzyme Reactions: Theory and Practice, Kodansha Ltd, Halsted Press, Tokyo, New York.
48. Abdullah, M., French, D. and Robyt, J. F., 1966. Arch. Biochem. Biophys. 114: 595–598.
49. Robyt, J. F. and French, D., 1967. Arch. Biochem. Biophys. 122: 8–16.
50. Rao, G. J. S. and Ramachandran, L. K., 1962. Biochim. Biophys. Acta 59: 507–508.
51. Hayashi, K., Imoto, T., Funatsu, G. and Funatsu, M., 1965. J. Biochem. (Tokyo) 58: 227–235.
52. Kawashima, S. and Ando, T., 1969. Int. J. Protein Research 1: 185–192.
53. Hiromi, K., Kawagishi, T. and Ohnishi, M., 1977. J. Biochem. (Tokyo) 81: 1583–1586.
54. Ohnishi, M., Taniguchi, M. and Hiromi, K. Biochim. Biophys. Acta (in press).
55. Taniguchi, M., 1980. Master's Thesis, Kyoto University.

Received 4 october 1982.